

Dynamic Pricing based Near-Optimal Resource Allocation for Elastic Edge Offloading

Yun Xia, Hai Xue, *Member IEEE*, Di Zhang, *Senior Member, IEEE*, Shahid Mumtaz, *Senior Member, IEEE*, Xiaolong Xu, *Senior Member, IEEE*, Joel J. P. C. Rodrigues, *Fellow, IEEE*

Abstract—In mobile edge computing (MEC), task offloading can significantly reduce task execution latency and energy consumption of end user (EU). However, edge server (ES) resources are limited, necessitating efficient allocation to ensure the sustainable and healthy development for MEC systems. In this paper, we propose a dynamic pricing mechanism based near-optimal resource allocation for elastic edge offloading. First, we construct a resource pricing model and accordingly develop the utility functions for both EU and ES, the optimal pricing model parameters are derived by optimizing the utility functions. In the meantime, our theoretical analysis reveals that the EU's utility function reaches a local maximum within the search range, but exhibits barely growth with increased resource allocation beyond this point. To this end, we further propose the Dynamic Inertia and Speed-Constrained particle swarm optimization (DISC-PSO) algorithm, which efficiently identifies the near-optimal resource allocation. Comprehensive simulation results validate the effectiveness of DISC-PSO, demonstrating that it significantly outperforms existing schemes by reducing the average number of iterations to reach a near-optimal solution by 92.11%, increasing the final user utility function value by 0.24%, and decreasing the variance of results by 95.45%.

Index Terms—DISC-PSO algorithm, dynamic pricing, elastic edge offloading, mobile edge computing, near-optimal resource allocation.

I. INTRODUCTION

IN remote areas, deploying diverse sensor devices (SDs) for environmental monitoring presents significant challenges due to the limited computational power and energy constraints of these SDs [1], [2]. When all data processing is conducted on-device, it rapidly depletes the SDs' batteries, thereby reducing their operational lifespan. To tackle this challenging issue,

This work was supported in part by the National Natural Science Foundation of China (NSFC) under Grant 62372242 and U22A0001, the Henan Natural Science Foundation for Excellent Young Scholar under Grant 242300421169, the Brazilian National Council for Scientific and Technological Development - CNPq via Grant No. 306607/2023-9. (*Corresponding author: Hai Xue.*)

Yun Xia and Hai Xue are with the School of Optical-Electrical and Computer Engineering, University of Shanghai for Science and Technology, Shanghai 200093, China (e-mail: xiadayun99@gmail.com, hxue@usst.edu.cn).

Di Zhang is with the School of Electrical and Information Engineering, Zhengzhou University, the Henan International Joint Laboratory of Intelligent Health Information System, the National Telemedicine Center, and the National Engineering Laboratory for Internet Medical Systems and Applications, Zhengzhou 450001, China (e-mail: dr.di.zhang@ieee.org).

Shahid Mumtaz is with the Department of Engineering, Nottingham Trent University, Nottingham NG1 4FQ, UK, and the Department of Electronic Engineering, Kyung Hee University, Yongin-si, Gyeonggi-do 17104, South Korea (e-mail: dr.shahid.mumtaz@ieee.org).

Xiaolong Xu is with the School of Software, Nanjing University of Information Science and Technology, Nanjing 210044, China (e-mail: xlxu@ieee.org).

Joel J. P. C. Rodrigues is with the Amazonas State University, Manaus - AM, Brazil (e-mail: joeljr@ieee.org).

offloading the computational tasks to cloud servers has been widely investigated. However, the physical distance between the SDs and cloud servers causes significant delay [3], [4], which is detrimental to delay-sensitive applications.

To mitigate the serious latency, mobile edge computing (MEC) has emerged as a promising computing paradigm. MEC enables the offloading of computational tasks to edge servers (ESs) situated closer to the SDs, which significantly reduces latency and energy consumption of the end devices [5], [6], [7]. In this way, it not only enhances the performance and efficiency of the sensor network but also extends the battery life of the SDs.

Nevertheless, ESs need incentives to participate in this process. Without appropriate compensation, ESs may be reluctant to offer their resources for task processing [8], [9]. Therefore, it is imperative to develop an efficient incentive mechanism to stimulate ESs to assist in task execution. Moreover, given the limited resources of ESs, adequately allocating these resources in the face of a large number of task offloading requests poses a significant challenge. Resource pricing as an incentive mechanism has garnered extensive attention in recent researches, since it has the potential to efficiently allocate resources and encourage participation from resource providers [10], [11], [12].

Therefore, in this paper, we explore the development of a dynamic pricing based resource allocation scheme, aiming to strike a balance between maximizing the utility of SDs while ensuring reasonable and fair resource allocation for ESs. To this end, we initially develop a dynamic pricing expression that relates ES resources to end users' (EU) data offloading amount. Based on the formulated pricing expression, a utility function for EU is constructed and its local maximum value is obtained by solving the utility function. Moreover, we theoretically analyzed and observed that the utility function exhibits barely growth near the local maximum value, indicating that limited benefits in allocating additional resources to EUs. Following that, a Dynamic Inertia and Speed-Constrained particle swarm optimization (DISC-PSO) algorithm is proposed to devise a near-optimal resource allocation scheme. Within a given precision range, DISC-PSO obtains near-optimal EU utility and derives corresponding near-optimal resource allocations. Furthermore, we prove that when the EU's utility function reaches the near-optimal level, so does the ES's utility, thus validating the effectiveness and rationality of the proposed DISC-PSO algorithm.

The key contributions of this paper are concluded as follows.

1) We develop a dynamic pricing scheme that takes into

account computing resources, bandwidth resources, and offloaded data amount. The proposed scheme exhibits an intuitive representation of the relationship between EU requirements and expenditures, while ensuring fair resource allocation among diverse EUs.

- 2) We formulate a utility function to quantify the benefits that EUs can derive from task offloading and their corresponding expenditures. Furthermore, we demonstrate that this utility function exhibits a local maximum, indicating that EUs can achieve optimal utility by appropriately balancing offloaded data amount with the acquisition of computing and bandwidth resources.
- 3) We theoretically analyzed and proved that the utility function grows barely while arriving near the local maximum value, even through allocating more resources. To this end, we propose the DISC-PSO algorithm to elucidate a near-optimal resource allocation scheme. Comprehensive simulation results demonstrate that the proposed DISC-PSO algorithm exhibits significant improvements compared to existing algorithms. Specifically, it reduced the number of iterations required to reach the near-optimal solution by an average of 92.11%, increased the final EU utility function value by 0.24%, and decreased the variance of the final results by 95.45%.
- 4) We conducted extensive simulations and theoretical analysis to validate the effectiveness of our proposed dynamic pricing scheme. The results reveal that it not only rationalizes resource pricing but also ensures the utilities of both EU and ES to reach their local maxima.

The rest of this paper is organized as follows. In Section II, we present the related works. Section III illustrates the proposed system model which includes the model of time and energy consumption, also exhibits the problem formulation and solutions. In Section IV, simulation results are presented and discussed. The conclusion is given in Section V.

II. RELATED WORK

Over the past few years, resource allocation based on pricing schemes has been extensively investigated, employing various specific methodologies, we summarized them into the three following categories.

A. Optimization algorithm-based resource allocation

A couple of researches [13], [14], [15], [16] have investigated the optimal resource allocation through the utilization of optimization algorithms. Huang *et al.* [13] proposed a hierarchical optimization algorithm for resource allocation, which decomposes the problem into three independent subproblems, and solves them by optimization algorithms such as genetic algorithm, and differential evolution algorithm. Zhou *et al.* [14] aimed to jointly optimize the decision of computation offloading, task offloading ratio, as well as the allocation of communication and computing resources, in order to minimize the overall cost of task processing for all EUs. The authors addressed this optimization problem by enhancing both the artificial fish swarm algorithm and the particle swarm optimization algorithm, resulting in efficient resource allocation

for communication and computing. Teng *et al.* [15] proposed a hybrid time-scale joint computation offloading and wireless resource allocation scheme, optimizing the offloading strategy and CPU frequency to achieve efficient resource allocation. They formulated a random convex optimization problem to optimize the offloading strategy and CPU frequency, utilizing the L0-norm as a representation of the offloading strategy. Moreover, the sample average approximation method was utilized to approximate the solution of this hybrid time-scale optimization problem. By adjusting both the offloading strategy and resource allocation scheme, the algorithm can effectively identify an optimal solution. Xiang *et al.* [16] proposed a modeling approach for multi-stage convex optimization problems to achieve efficient resource allocation. The authors transformed the problem of cost-effective service provision into a multi-stage convex optimization problem, thereby optimizing the resource allocation. Additionally, they proposed an online algorithm RDC based on the Lyapunov framework, which decomposes the entire problem into multiple subproblems to facilitate resource allocation.

B. Stackelberg game-based resource allocation

Several papers [17], [18], [19] have employed Stackelberg game theory to achieve optimal resource allocation. Cheng *et al.* [17] conducted resource allocation within the framework of a Stackelberg game, and proposed two distinct schemes for pricing and resource allocation: one based on user granularity and the other on task granularity. By employing the backward induction method, edge servers determine the optimal strategy for pricing and resource allocation based on EUs' responses. Ahmed *et al.* [18] introduced a dynamic resource allocation method based on Stackelberg game theory, enabling efficient utilization of multiple MEC servers. Specifically, the authors formulated a comprehensive Stackelberg game model to analyze pricing and resource procurement challenges faced by MEC servers. In addition, they devised an algorithm for multi-to-multi resource sharing among MEC servers. They also developed a separate algorithm for one-to-many resource allocation between MEC servers and edge service providers. Li *et al.* [19] employed a multi-stage Stackelberg game for achieving resource allocation, wherein vehicles are incentivized to share their idle resources through reasonable contracts. Additionally, the interaction among roadside units, MEC servers, and mobile device EUs is modeled using the Stackelberg game to attain effective resource allocation and computation task offloading decisions. The optimal strategy for each stage is obtained via the backward induction method, thereby optimizing resource allocation.

C. Auction-based resource allocation

Auction mechanisms have also been utilized in existing researches [20], [21], [22], [23], [24], [25] for the purpose of resource allocation. Habiba *et al.* [20] proposed a repeated auction model for resource allocation, wherein MEC servers and EU devices participated in bidding, and the final resource allocation was determined by the bidding results. To be specific, they designed a modified generalized second

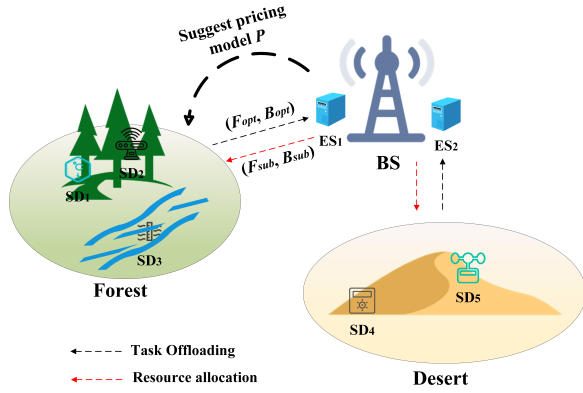


Fig. 1: System model.

price algorithm to set pricing and allocate resources, taking into account the dynamic arrival of offloading requests and the computing workloads of ESs. Sun *et al.* [21] devised a bid-based two-sided auction framework wherein mobile devices compete for computing services while edge servers offer such service through bidding. Within this framework, the authors also proposed two specific two-sided auction schemes: cost balancing and dynamic pricing, thereby achieving efficient resource allocation. Bahreini *et al.* [22] proposed two auction-based resource allocation and pricing mechanisms, namely FREAP and APXERAP. FREAP employs a greedy approach, while APXERAP utilizes linear programming as an approximation technique. Both mechanisms consider the heterogeneity of EU requests and resource types, resulting in resource allocation and pricing strategies that closely approximate optimal social welfare. Wang *et al.* [23] proposed an auction-based resource allocation mechanism that considers the flexibility and locality of task offloading, enabling joint allocation of computing and communication resources as well as partial offloading. The mechanism achieves efficient resource allocation and enhances social welfare by integrating a minimum delay task graph partitioning algorithm, a feasible non-dominated resource allocation determination algorithm, and an original-dual approximate winning bid selection algorithm. Li *et al.* [24] utilized a two-sided auction mechanism to achieve resource allocation. Specifically, the authors proposed two two-sided auction mechanisms, namely TMF and EMF, to optimize both rationality in resource allocation and social welfare considering the successful transactions. Li *et al.* [25] proposed a double auction game model to address the resource management problem in MEC and Internet of Things (IoT) devices. In this mechanism, MEC acts as seller while IoT devices act as buyers, submitting their bids and offers. The auction intermediary determines the transaction price based on participants' submissions, establishing a fair and effective market for resource transactions. The experience-weighted attraction algorithm is proposed to enhance the learning process of transaction strategies and find the Nash equilibrium point.

However, current pricing-based resource allocation schemes encounter certain issues. Existing researches [17], [21], [24], [25] simplify the representation of resources and assign ab-

stract prices to them, which may facilitate problem-solving but fail to accurately reflect the actual and precise resource requirements of EUs. Moreover, both optimization algorithm-based resource allocation and Stackelberg game-based resource allocation suffer from the drawback that the price is determined during the optimization process or game [13], [14], [15], [16], [17], [18], [19], thereby rendering it transparent to EUs before their purchase. Consequently, this fails to align with the genuine resource needs of EUs. In the auction process described in [20], [21], [22], [23], [24], [25], although EUs are aware of their bids, multiple rounds of auctions are required for finalizing the resource allocation outcome, inevitably resulting in serious time consumption.

III. SYSTEM MODEL AND PROBLEM FORMULATION

A. System model

As depicted in Fig. 1, we consider the resource allocation problem between single EU and ES in remote area (e.g., forest, desert). It is known that when the EU offloads data to the ES, it can reduce energy consumption. The more ES resources they purchase (e.g., computational frequency F and bandwidth B), the faster the tasks are processed and returned. Therefore, the EU needs to decide how much F and B to purchase. First, the ES provides a pricing model of P . Then, the EU constructs a utility function $U_{user}(P, F, B)$ and maximizes it to determine the optimal amount of resources (F_{opt}, B_{opt}) to purchase. However, when the offloaded data amount is fixed, the increase of EU's utility becomes negligible as the purchased resources increase¹. To rationalize resource allocation, the ES, based on the EU-provided (F_{opt}, B_{opt}) will determine a near-optimal resource allocation (F_{sub}, B_{sub}) within an acceptable range of the maximum utility function U_{user}^{max} . For the sake of convenience, Table I summarizes the important notations in this paper.

B. Time consumption model

We define the amount of EU's offloading data as q , the number of CPU cycles required to process each bit of data as c , and the EU's local CPU frequency as F_{local} . Therefore, the EU's local data execution time is calculated as follows.

$$T_{local} = \frac{qc}{F_{local}}. \quad (1)$$

Since there are different signal-to-noise ratios $(S/N)_{uplink}$ and $(S/N)_{downlink}$ for the uplink and downlink transmission, different uplink and downlink transmission speed R_u and R_d is obtained respectively according to Shannon's formula.

$$R_u = B \log_2 \left(1 + \left(\frac{S}{N} \right)_{uplink} \right), \quad (2)$$

$$R_d = B \log_2 \left(1 + \left(\frac{S}{N} \right)_{downlink} \right), \quad (3)$$

¹Considering that the amount of offloaded data is constant, initial resource increase results in a substantial reduction in latency and energy consumption, leading to a noticeable improvement in utility. However, as more resources are supplied, the impact of these reductions becomes less pronounced, and the marginal gains in utility diminish.

TABLE I: SUMMARY OF PRIMARY NOTATIONS

Symbol	Description
q	The maximum amount of data offloading of the EU
c	The number of cycles required to process a bit
F_{local}	The local CPU frequency of EU
T_{local}	The local time of processing data
B	The bandwidth resources purchased by EU
R_u	The speed of uplink transmission
R_d	The speed of downlink transmission
T_u	The time of uplink transmission
T_d	The time of downlink transmission
T_p	The time of processing data on ES
α	The data conversion ratio
k	The effective switched capacitance
F_{server}	The ES CPU frequency purchased by EU
E_{up}	The amount of energy consumed by uploading task
E_d	The amount of energy consumed by downloading task
w_1	The discount factor of time-saving
w_2	The discount factor of energy-saving

where B is the bandwidth purchased by the EU. Thus the uplink transmission time T_u is expressed as follows.

$$T_u = \frac{q}{R_u}. \quad (4)$$

Assuming that the CPU frequency of ES computation purchased by the EU is F_{server} . Then, the time T_p of data processing on the ES is expressed as follows.

$$T_p = \frac{qc}{F_{server}}. \quad (5)$$

Since the download data is relatively less compared to the amount of uploaded data, we assume the conversion ratio as α [38]. Therefore, the downlink transmission time T_d is illustrated as follows.

$$T_d = \frac{\alpha q}{R_d}. \quad (6)$$

To sum up, the total time of the entire process for EU offloading data to the ES includes the uplink transmission time T_p , the downlink transmission time T_d , and the execution time T_p of the ES. Accordingly, the total offloading time $T_{offload}$ is calculated as follows,

$$\begin{aligned} T_{offload} &= T_u + T_p + T_d \\ &= \frac{q}{R_u} + \frac{qc}{F_{server}} + \frac{\alpha q}{R_d} \\ &= q \cdot \left(\frac{1}{R_u} + \frac{c}{F_{server}} + \frac{\alpha}{R_d} \right). \end{aligned} \quad (7)$$

Therefore, the time T_{save} saved by offloading versus non-offloading is illustrated as follows.

$$\begin{aligned} T_{save} &= T_{local} - T_{offload} \\ &= \frac{qc}{F_{local}} - q \cdot \left(\frac{1}{R_u} + \frac{c}{F_{server}} + \frac{\alpha}{R_d} \right) \\ &= q \cdot \left(\frac{c}{F_{local}} - \frac{1}{R_u} - \frac{c}{F_{server}} - \frac{\alpha}{R_d} \right). \end{aligned} \quad (8)$$

C. Energy consumption model

If the EU processes q bit data locally, the required energy consumption E_{local} is calculated by the following expression [27].

$$E_{local} = k \cdot (qc) \cdot F_{local}^2, \quad (9)$$

where k is an energy consumption coefficient that depends on the chip architecture. The energy consumed by EU in the offloading process includes the energy consumption E_{up} of uploading data, and the energy consumption E_d of downloading data.

$$E_{up} = P_u \cdot T_u, \quad (10)$$

$$E_d = P_d \cdot T_d, \quad (11)$$

where P_u and P_d are the power of the EU for uploading and downloading data, respectively. Therefore, the energy E_{save} saved by the EU in the offloading process is shown as follows.

$$\begin{aligned} E_{save} &= E_{local} - E_{up} - E_d \\ &= k \cdot (qc) \cdot F_{local}^2 - P_u \cdot T_u - P_d \cdot T_d \\ &= q \cdot \left(kcF_{local}^2 - \frac{P_u}{R_u} - \frac{P_d \cdot \alpha}{R_d} \right). \end{aligned} \quad (12)$$

D. Validation function of EU

As the original intention of edge offloading, EUs offload tasks to save energy and reduce latency. However, during this process, EUs must also cover the cost of acquiring resources from the ES to ensure proper functioning and support. Thus we can define the EU's utility function U_{user} as follows.

$$U_{user} = w_1 \cdot E_{save} + w_2 \cdot T_{save} - P, \quad (13)$$

where w_1 and w_2 denote the discount factors of time-saving and energy-saving [28], respectively, which denote the EU in favor of time or energy consumption. In addition, the payment function P is positively correlated to the purchase of bandwidth resource B and the computing frequency F_{server} [29]. For convenience, we let the payoff function P satisfy the following expression.

$$P = a \cdot F_{server} + b \cdot B, \quad (14)$$

where $a > 0$ and $b > 0$. Then, substituting Eq.(2), Eq.(3), Eq.(8), Eq.(12), and Eq.(14) into Eq.(13), we obtain the following expression.

$$\begin{aligned} U_{user} &= w_1 \left(q \cdot \left(kcF_{local}^2 - \frac{P_u}{B \log_2 \left(1 + \left(\frac{S}{N} \right)_{uplink} \right)} \right. \right. \\ &\quad \left. \left. - \frac{P_d \cdot \alpha}{B \log_2 \left(1 + \left(\frac{S}{N} \right)_{downlink} \right)} \right) \right) + w_2 \left(q \cdot \left(\frac{c}{F_{local}} \right. \right. \\ &\quad \left. \left. - \frac{1}{B \log_2 \left(1 + \left(\frac{S}{N} \right)_{uplink} \right)} - \frac{c}{F_{server}} \right. \right. \\ &\quad \left. \left. - \frac{\alpha}{B \log_2 \left(1 + \left(\frac{S}{N} \right)_{downlink} \right)} \right) \right) \\ &\quad - (a \cdot F_{server} + b \cdot B) \\ &= q \cdot \left(w_1 kcF_{local}^2 + \frac{w_2 c}{F_{local}} \right) - \frac{q}{F_{server}} \cdot w_2 c \\ &\quad - \frac{q}{B} \left(\frac{w_1 P_u + w_2}{\log_2 \left(1 + \left(\frac{S}{N} \right)_{uplink} \right)} + \frac{w_1 P_d \alpha + w_2 \alpha}{\log_2 \left(1 + \left(\frac{S}{N} \right)_{downlink} \right)} \right) \\ &\quad - a F_{server} - b B. \end{aligned} \quad (15)$$

To simplify the expression of U_{user} , we let

$$\mathcal{X} = w_1 k c F_{local}^2 + \frac{w_2 c}{F_{local}}, \quad (16)$$

$$\mathcal{Y} = \frac{w_1 P_u + w_2}{\log_2(1 + (\frac{S}{N})_{uplink})} + \frac{w_1 P_d \alpha + w_2 \alpha}{\log_2(1 + (\frac{S}{N})_{downlink})}. \quad (17)$$

Substituting \mathcal{X} and \mathcal{Y} into Eq.(15) yields the following expression.

$$U_{user} = q \cdot \mathcal{X} - \frac{q}{F_{server}} \cdot w_2 c - \frac{q}{B} \cdot \mathcal{Y} - a F_{server} - b B. \quad (18)$$

We take the first partial and second partial derivations for F_{server} and B , respectively. Then, we obtain the following expressions.

$$\frac{\partial U_{user}}{\partial F_{server}} = \frac{w_2 c q}{F_{server}^2} - a, \quad (19)$$

$$\frac{\partial U_{user}}{\partial B} = \frac{q \mathcal{Y}}{B^2} - b, \quad (20)$$

$$\frac{\partial^2 U_{user}}{\partial^2 F_{server}} = -\frac{2 w_2 c q}{F_{server}^3}, \quad (21)$$

$$\frac{\partial^2 U_{user}}{\partial^2 B} = -\frac{2 q \mathcal{Y}}{B^3}, \quad (22)$$

$$\frac{\partial^2 U_{user}}{\partial F_{server} \partial B} = 0, \quad (23)$$

$$\frac{\partial^2 U_{user}}{\partial B \partial F_{server}} = 0. \quad (24)$$

The Hessian matrix is classically utilized to determine the critical points of a function for optimization issues [30], [31], [32]. Therefore, we construct the Hessian matrix \mathcal{H} using Eq.(21), Eq.(22), Eq.(23), and Eq.(24).

$$\begin{aligned} \mathcal{H} &= \begin{bmatrix} \frac{\partial^2 U_{user}}{\partial^2 F_{server}} & \frac{\partial^2 U_{user}}{\partial F_{server} \partial B} \\ \frac{\partial^2 U_{user}}{\partial B \partial F_{server}} & \frac{\partial^2 U_{user}}{\partial^2 B} \end{bmatrix} \\ &= \begin{bmatrix} -\frac{2 w_2 c q}{F_{server}^3} & 0 \\ 0 & -\frac{2 q \mathcal{Y}}{B^3} \end{bmatrix}. \end{aligned} \quad (25)$$

Lemma 1: \mathcal{H} is a negative definite matrix.

Proof 1: please see the appendix A for details.

From Lemma 1, we can know that the Hessian matrix \mathcal{H} of U_{user} is a negative definite matrix, which means the U_{user} has a local maximum value at critical point². We let Eq.(19) and Eq.(20) equal to 0, and then we can find the critical point (F_{server}, B) as follows.

$$\begin{cases} F_{server} = \sqrt{\frac{w_2 c q}{a}}, \\ B = \sqrt{\frac{q \mathcal{Y}}{b}}. \end{cases} \quad (26)$$

Lemma 2: U_{user} hardly increases while approximating the local maximum.

Proof 2: please see the appendix B for details.

Eq.(26) illustrates that when the EU offloads q bit data, how many computational frequency and bandwidth resources of the

edge server to be purchased, so as to maximize its own utility function. Therefore, by substituting Eq.(26) into Eq.(18), the final expression for U_{user} is obtained.

$$U_{user} = q \cdot \mathcal{X} - \frac{2 q}{F_{server}} \cdot w_2 c - \frac{2 q}{B} \cdot \mathcal{Y}. \quad (27)$$

E. Validation function of ES

In edge computing environment, offloading tasks to the ES necessitates the use of ES resources to process the computations. Since the ES requires compensation for providing these resources, the EU must pay fees to offload its task effectively. At the same time, for the ES, it takes time to process the EU's task, which means that the ES has a time cost³. The less time the ES spends on processing EU tasks, the lower the cost. In addition, when the ES processes the EU's data, it also obtains the EU's data, and these data also bring revenue W to the ES [35]. So the utility function of the ES is obtained as follows.

$$U_{server} = P - T_{offload} + W. \quad (28)$$

We substitute Eq.(26) into Eq.(14) to obtain the expression for P as follows.

$$P = \frac{w_2 c q}{F_{server}} + \frac{q \mathcal{Y}}{B}. \quad (29)$$

Inspired by [36] and [37], we define W as the following expression.

$$W = \mu \log_2(1 + q), \quad (30)$$

where $\mu \in (0, 1)$ denotes the reward index. Substituting Eq.(7), Eq.(29) and Eq.(30) into Eq.(28) yields the following expression.

$$\begin{aligned} U_{server} &= \frac{w_2 c q}{F_{server}} + \frac{q \mathcal{Y}}{B} - q \cdot \left(\frac{1}{R_u} + \frac{c}{F_{server}} + \frac{\alpha}{R_d} \right) \\ &+ \mu \log_2(1 + q) \\ &= \frac{c q (w_2 - 1)}{F_{server}} + \frac{q}{B} \left(\frac{w_1 P_u + w_2 - 1}{\log_2(1 + (\frac{S}{N})_{uplink})} \right. \\ &\left. + \frac{w_1 P_d \alpha + w_2 \alpha - \alpha}{\log_2(1 + (\frac{S}{N})_{downlink})} \right) + \mu \log_2(1 + q). \end{aligned} \quad (31)$$

F. Server optimal policy

As aforementioned, Lemma 2 proves that U_{user} hardly increases while approximating the local maximum. Given the efficient and rational utilization of server resources, we pick the near-optimal resource allocation. When the utility functions of both ES and EU remain fairly constant within a certain resource allocation range, we allocate fewer resources, which is beneficial for saving resources and allowing the ES to serve more EUs over a while. We define the allocation strategy (F_{sub}, B_{sub}) as a near-optimal allocation if the condition $\frac{U_{max} - U_{sub}}{U_{sub}} < \epsilon$ is satisfied, where U_{max} is the optimal utility within the search space, U_{sub} is the utility achieved under the

³Here, even if ES does not process EU data, it still requires a significant amount of energy to operate. The energy expended in processing EU data is relatively small compared to this, so we ignore energy consumption costs. Additionally, some papers [18], [33], [34] also do not include energy consumption as part of the ES utility function.

²The local maximum within the search space is treated as a global maximum in our analysis, since there is no global maximum of U_{user} , resulting in the globally optimal allocation.

TABLE II: SUMMARY OF PRIMARY NOTATIONS FOR ALGORITHM 1

Symbol	Description
P_n	The number of particles
w_{max}	The maximum inertia weight
w_{min}	The minimum inertia weight
c_1	The individual learning factor
c_2	The social learning factor
ΔF	The minimum change value of F_{server}
ΔB	The minimum change value of B
$[F_{server}^{min}, F_{server}^{max}]$	The search range of F_{server}
$[B_{min}, B_{max}]$	The search range of B
N_t	The number of experiments
N_{max}	The maximum number of iterations
N_f	The number of actual iterations
P_{pos}	The position of particles
V	The velocity of particles
P_{pb}	The best position for each particle
P_{bs}	The best U_{user} for each particle
S_{gb}	The largest U_{user} of all particles
I_{bp}	The index corresponding to S_{gb}
P_{gb}	The best position of all particles

allocation scheme (F_{sub}, B_{sub}), and ϵ is a predefined threshold value. For this reason, we propose a DISC-PSO algorithm as illustrated in algorithm 1 to seek this near-optimal resources allocation point (F_{server}, B) through continuous iterations. Primary notations involved in algorithm 1 are summarized in Table II. First, we obtain the EU's maximum utility U_{user}^{max} through Eq.(26) (i.e., the critical point). Initialization is performed at the same time, including the P_{pos}, V, P_{pb} , and $A_s[P_n][1]$ for all particles, while recording S_{gb} and P_{gb} in all particles (see line 2 to 8 of algorithm 1). It then goes into an iteration, updating the V and P_{pos} , while ensuring that ΔF and ΔB are satisfied (see line 12 to 21 of algorithm 1). Then we update the P_{pb} and $A_s[P_n][1]$. If there are values in the matrix $A_s[P_n][1]$ greater than S_{gb} , then we update the P_{gb} and S_{gb} (see line 23 to 33 of algorithm 1). Subsequently, it is judged whether the termination condition as shown in Eq.(32) is satisfied. If so, the iteration process is terminated (see line 35 to 36 of algorithm 1). Finally, the experimental results included S_{gb}, N_f , and P_{gb} are recorded.

$$\frac{U_{user}^{max} - S_{gb}}{S_{gb}} < \epsilon. \quad (32)$$

In comparison with the traditional PSO algorithm, our proposed DISC-PSO algorithm is enhanced from the following aspects to accelerate the convergence speed: 1). We change the inertia weight w from fixed value to dynamic change (see line 14 of algorithm 1); 2). We add the condition limiting the minimum change in speed (see line 16 to line 17 of algorithm 1); 3). In addition to reaching the maximum number of iterations to stop iteration, we also add the termination condition of Eq.(32) (see line 35 to line 36 of algorithm 1). The time complexity of the DISC-PSO algorithm is analyzed as follows:

- The outer loop runs for N_t iterations, which represents the number of experiments conducted.
- The inner loop (i.e., lines 10-36) is executed up to N_{max} times, representing the maximum number of iterations for particle updates.
- Within the inner loop, the for-loop (i.e., lines 11-21) iterates over P_n particles, and each particle's position and velocity are updated in $O(1)$ time. The complexity for this section is $O(P_n)$.
- The update of personal and global bests (i.e., lines 23-33) also requires $O(P_n)$.
- The stopping condition check (i.e., line 35) takes $O(1)$ time.

Given the nested loops, the overall time complexity of the algorithm is $O(N_t \times N_{max} \times P_n)$, which represents the worst-case scenario where the algorithm runs through all possible iterations.

TABLE III: DEFAULT PARAMETER SETTINGS

Parameter	Value	Parameter	Value
c	2640 <i>cycles/bit</i>	P_d	1W
F_{server}	{1, 2, ..., 6}GHz	P_u	0.1W
μ	0.8	w_1, w_2	0.5
F_{local}	{0.1, 0.2, ..., 1}GHz	$(S/N)_{uplink}$	20dB
q	[100, 500] KB	$(S/N)_{downlink}$	30dB
k	$10^{-27} Watt \cdot s^3 / cycles^3$	α	0.2
B	{0.1, 0.2, ..., 1}Mbps	ϵ	0.001

IV. PERFORMANCE EVALUATION

In this section, in order to verify the effectiveness and rationality of the proposed dynamic pricing scheme, we explore the pricing (i.e., P), the corresponding U_{user} and U_{server} with varying resource allocations (i.e., F_{server} and B). Furthermore, we analyze the near-optimal value of the EU utility function with the proposed DISC-PSO algorithm, which demonstrates advantages in terms of efficiency, stability, and solution quality compared to existing algorithms. It should be noted that optimizing the EU utility function inherently results in the optimization of the ES utility function, as proven in Appendix C. This ensures that the proposed resource allocation scheme effectively optimizes both utilities, allowing us to focus primarily on the EU utility in the subsequent analysis without reiterating the equivalence.

A. Simulation Setup

For the simulation setup, the local CPU frequency F_{local} of each EU is uniformly selected from the set {0.1, 0.2, ..., 1} GHz, $\alpha = 0.2$, $P_u = 0.1W$, and $P_d = 1W$ [38]. In addition, the data size of EU is uniformly distributed with $q \in [100, 500]$ KB [39]. The remaining parameter settings are summarized in Table III [29], [40], [41].

B. The effect of F_{server} on P, U_{user} , and U_{server} .

As shown in Fig. 2, we explore the resource pricing P , the EU utility function U_{user} , and the ES utility function U_{server} with different F_{server} purchased by EUs. We set the bandwidth resource of the EU to buy $B = 0.1Mbps$, as well as the

Algorithm 1: DISC-PSO

Input: $P_n, w_{max}, w_{min}, c_1, c_2, \Delta F, \Delta B, [F_{server}^{min}, F_{server}^{max}], [B^{min}, B^{max}], N_t, N_{max}, \epsilon$

Output: S_{gb}, N_f, P_{gb}

```

1 for  $exp = 1: N_t$  do
2   Substitute Eq.(26) into Eq.(13) to obtain the
   maximum value  $U_{user}^{max}$ ;
3    $P_{pos} = [F_{server}^{min} + (F_{server}^{max} - F_{server}^{min}) \times \text{rand}(P_n,$ 
    $1), B^{min} + (B^{max} - B^{min}) \times \text{rand}(P_n, 1)];$ 
4    $V = \text{zeros}(P_n, 2);$ 
5    $P_{pb} \leftarrow P_{pos};$ 
6   Calculate  $U_{user}$  for the current position of each
   particle and record it in the matrix  $A_s[P_n][1];$ 
7    $[S_{gb}, I_{bp}] \leftarrow \max(A_s[P_n][1]);$ 
8    $P_{gb} = P_{pb}(I_{bp}, :);$ 
9    $N_f = 0;$ 
10  while  $N_f < N_{max}$  do
11    for  $i = 1: P_n$  do
12       $r_1 = \text{rand};$ 
13       $r_2 = \text{rand};$ 
14       $w = w_{max} - ((w_{max} - w_{min}) \times N_f / N_{max})$ 
      ;
15       $V(i, :) = w \times V(i, :) + c_1 \times r_1 \times (P_b(i, :$ 
       $) - P_{pos}(i, :)) + c_2 \times r_2 \times (P_{gb} - P_{pos}(i, :));$ 
16       $V(i, 1) =$ 
       $\text{sign}(V(i, 1)) \times \max(\text{abs}(V(i, 1)), \Delta F);$ 
17       $V(i, 2) =$ 
       $\text{sign}(V(i, 2)) \times \max(\text{abs}(V(i, 2)), \Delta B);$ 
18       $P_{pos}(i, :) = P_{pos}(i, :) + V(i, :);$ 
19       $P_{pos}(i, 1) = \max(F_{server}^{min};$ 
       $\min(F_{server}^{max}, P_{pos}(i, 1)));$ 
20       $P_{pos}(i, 2) =$ 
       $\max(B^{min}, \min(B^{max}, P_{pos}(i, 2)));$ 
21    end
22     $S = A_s[P_n][1];$ 
23    for  $i = 1: P_n$  do
24      if  $S(i) > A_s[P_n][1](i)$  then
25         $A_s[P_n][1](i) = S(i);$ 
26         $P_{pb}(i, :) = P_{pos}(i, :);$ 
27      end
28    end
29  end
30   $[S_{ngb}, I_{bp}] = \max(A_s[P_n][1]);$ 
31  if  $S_{ngb} > S_{gb}$  then
32     $S_{gb} = S_{ngb};$ 
33     $P_{gb} = P_{pb}(I_{bp}, :);$ 
34  end
35  if  $\text{abs}(S_{gb} - U_{user}^{max}) / S_{gb} < \epsilon$  then
36    break;
37  end
38   $N_f = N_f + 1;$ 
39 end
40 Record  $S_{gb}, P_{gb},$  and  $N_f;$ 
41 end

```

amount of offloaded data 500KB. In addition, we denote F vary from 1GHz to 6GHz.

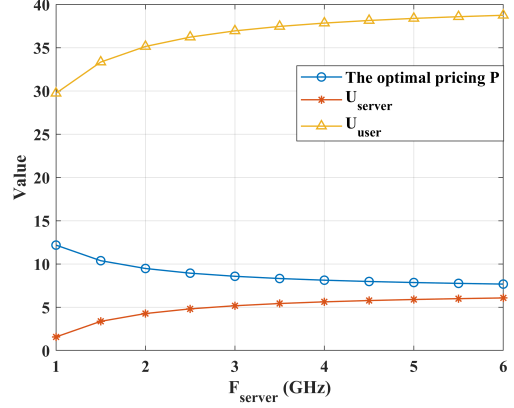


Fig. 2: Effect of F_{server} on P , U_{user} , and U_{server} .

From Fig. 2, it is observed that as F_{server} increases, P decreases and then becomes stable, while U_{user} as well as U_{server} increase and become stable. Firstly, Eq.(29) reflects the inverse relationship between P and F_{server} . As a result, the increase in F_{server} causes P to fall and flatten out. This also verifies the effectiveness of the proposed pricing model, which can motivate EUs to offload tasks more effectively. Secondly, based on the analysis of P , we analyze U_{user} and U_{server} as follows: for U_{user} , the increase of F_{server} accelerates the data processing speed. That is, the increase of T_{save} and the decrease of P lead to the increase of U_{user} according to Eq.(13). In addition, Eq.(8) reflects the inverse relationship between F_{server} and T_{save} , which leads to the flattening of U_{user} , as directly reflected in Eq.(27). Similarly, Eq.(7) indicates that F_{server} and $T_{offload}$ are inversely proportional, which implies that an increase in F_{server} reduces $T_{offload}$. Moreover, Eq.(31) demonstrates that an increase in F_{server} results in a corresponding increase in U_{server} .

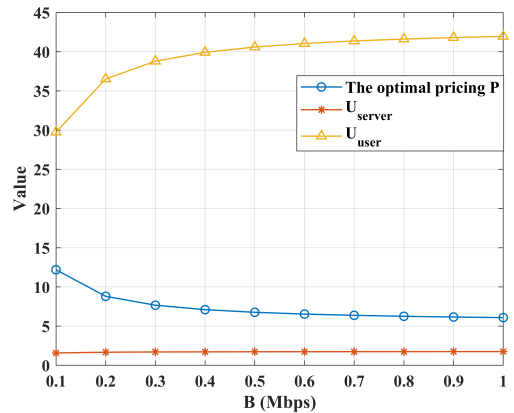


Fig. 3: Effect of B on P , U_{user} , and U_{server} .

C. The effect of B on P , U_{user} , and U_{server} .

As exhibited in Fig. 3, we explore P , U_{user} , and U_{server} with diverse B purchased by EUs. We set the CPU frequency resource for the EU to buy $F_{server} = 1GHz$, as well as the

amount of offloaded data $500KB$, and we let B vary from $0.1Mbps$ to $1Mbps$.

From Fig. 3, it can be seen that as B increases, P decreases and becomes stable, U_{user} increases and becomes stable while U_{server} keeps intact. By examining Eq.(27) and Eq.(29), we observe that the effect of B on P and U_{user} is analogous to that of F . As this impact has already been analyzed in Subsection B of Section IV, the same reasons also apply to B . However, for U_{server} , although the increase of B decreases $T_{offload}$, P also decreases accordingly. Thus, there is essentially no discernible change. In addition, by observing Eq.(31), we can see that part of the expression related to B is extracted as follows.

$$B_{part} = \frac{w_1 P_u + w_2 - 1}{\log_2(1 + (\frac{S}{N})_{uplink})} + \frac{w_1 P_d \alpha + w_2 \alpha - \alpha}{\log_2(1 + (\frac{S}{N})_{downlink})}. \quad (33)$$

By substituting the data in Table III, we calculate $B_{part} \approx -0.0676$, which represents a relatively small quantity. Therefore, no matter how B changes (i.e., in Eq.(31), B is the denominator while B_{part} is the numerator), the overall change is inconspicuous, which further verifies the stable phenomenon of U_{server} .

D. The effect of q on P , U_{user} , and U_{server}

As depicted in Fig. 4, we explore P , U_{user} , and U_{server} with different q offloaded by EUs. We set the CPU frequency resource for the EU to buy as $F_{server} = 6GHz$, as well as the bandwidth resource as $B = 1Mbps$, and we let q vary from $100KB$ to $500KB$.

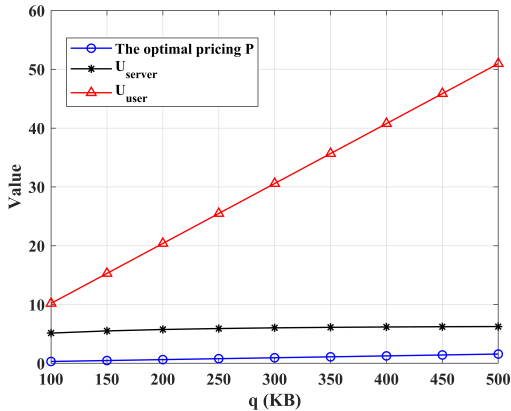


Fig. 4: Effect of q on P , U_{user} , and U_{server} .

As q increases, the U_{user} increases while U_{server} and P do not change markedly. For U_{server} , the growth rate from the point (100, 5.14252) to (500, 6.25469) is approximately 0.00278, while for P , the growth rate from (100, 0.315874) to (500, 1.57937) is approximately 0.00316. With respect to U_{user} , when the offloaded data amount gets larger, the E_{save} and T_{save} generated by ES become more obvious due to the constraint and miniature F_{local} . Therefore, the U_{user} becomes large, and this trend is intuitively reflected by Eq.(27). Similar

to the analysis of Eq.(33), we extract the expressions related to q in P as follows.

$$P_{part} = \frac{w_2 c}{F_{server}} + \frac{\mathcal{Y}}{B}. \quad (34)$$

By substituting the values in Table III into the expression, we can calculate that $P_{part} \in [3.227 \times 10^{-7}, 2.347 \times 10^{-6}]$, which is a small number, which explains P does not change much. Therefore, according to Eq.(28), the expression affecting U_{server} is illustrated as follows.

$$U_{affect} = -T_{offload} + W - q \cdot \left(\frac{1}{R_u} + \frac{c}{F_{server}} + \frac{\alpha}{R_d} \right) + \mu \log_2(1 + q). \quad (35)$$

Similarly, we substitute the values in Table III into the expression. That is, as q changes, U_{affect} does not change much. Therefore, U_{server} maintains a steady level.

E. The effect of F_{local} on P , U_{user} , and U_{server} .

As shown in Fig. 5, we explore P , U_{user} , and U_{server} under different F_{local} of EUs. We set the CPU frequency resource for the EU to buy as $F_{server} = 6GHz$, as well as the bandwidth resource as $B = 1Mbps$, and let $q = 500KB$.

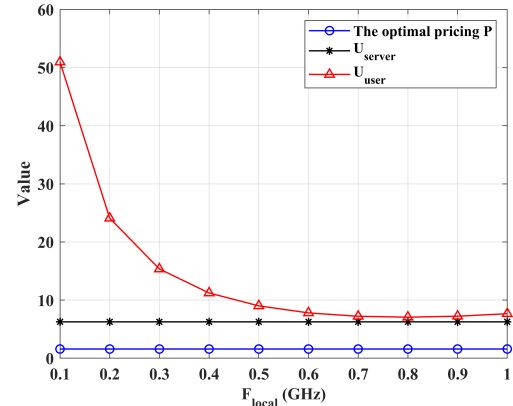


Fig. 5: Effect of F_{local} on P , U_{user} , and U_{server} .

As F_{local} increases, U_{user} begins to decrease while U_{server} and P do not change markedly. When F_{local} increases, the EU is more inclined to execute the task locally, resulting in a decrease in T_{save} , which leads to a decrease in the U_{user} . In addition, by observing Eq.(27), we can get the following expression.

$$U_{user} \propto \mathcal{X} = \mathcal{M} \cdot F_{local}^2 + \mathcal{N} \cdot \frac{1}{F_{local}}, \quad (36)$$

where $\mathcal{M} = w_1 k c$, and $\mathcal{N} = w_2 c$. Thus, the analysis of Eq.(36) also leads to the conclusion that U_{user} first decreases and then slightly increases. Since P and U_{server} are not related to F_{local} , P , and U_{server} remain unchanged.

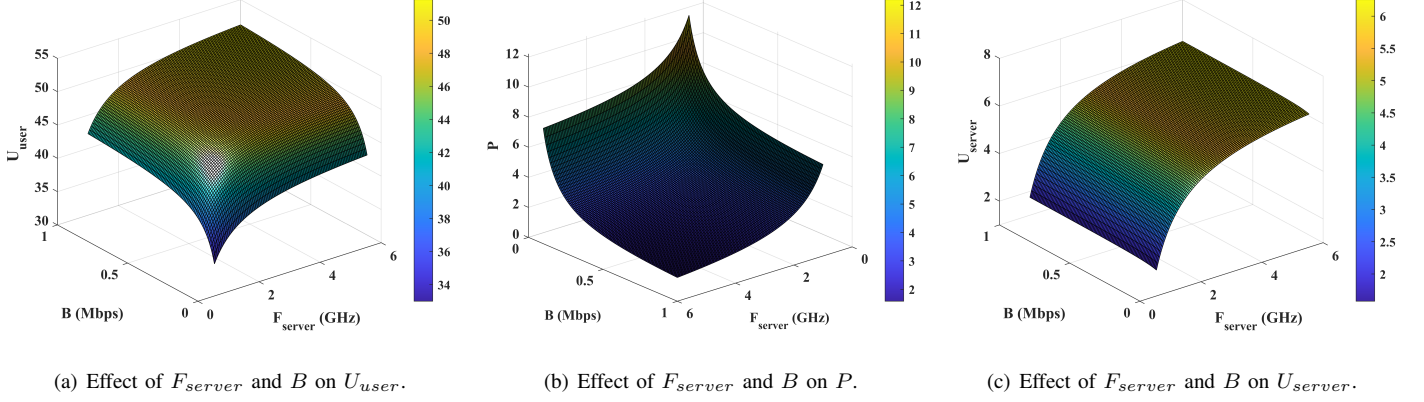


Fig. 6: Effect of F_{server} and B on U_{user} , P , and U_{server} .

F. The effect of F_{server} and B on U_{user} , P , and U_{server} .

In addition, we also analyze the U_{user} , P , and U_{server} for different F_{server} and B , as shown in Fig. 6. We set the bandwidth resource purchased by the EU $B \in [0.1Mbps, 1Mbps]$, the CPU frequency $F \in [1GHz, 6GHz]$, and the amount of offloaded data q as $500KB$.

From Fig. 6(a), it is observed that the U_{user} arrives at a local maximum at the point $(1Mbps, 6GHz)$, which is also confirmed by Eq.(26). In addition, with the increase of resource allocation, U_{user} gradually becomes stable. This prevents EUs from excessively seizing ES resources to boost U_{user} . As a result, ES resources are allocated and utilized more reasonably. As shown in Fig. 6(b), P gradually decreases as resource allocation increases. This observation is consistent with the trends illustrated in Fig. 2 and Fig. 3. The proposed pricing model effectively incentivizes EUs to offload tasks by reducing prices as more resources are purchased. This not only validates the effectiveness of the pricing scheme but also enhances overall system performance, since it encourages EUs to acquire additional computational resources, accelerating task execution and enhancing system efficiency.

Besides, as we can see from Fig. 6(c), the U_{server} tends to stabilize as the resources allocated to the EU reach a certain level, which is typically achieved when F_{server} exceeds $5GHz$. This limits the ES's ability to increase its U_{server} by over-selling resources to a single affluent EU, allowing the ES to allocate resources to EUs appropriately.

G. Near-optimal resource allocation with DISC-PSO algorithm

Next, we conducted 50 simulation runs to compare the U_{user} of seeking near-optimal value with different algorithms (i.e., as shown in Fig. 7), the corresponding number of iterations (i.e., as shown in Fig. 8), and the corresponding resource distribution (i.e., as shown in Fig. 9). In addition, we have carried out statistics on the physical quantities as shown in Table IV.

From Fig. 7, it can be seen that the U_{user} of the DISC-PSO is always at a high value and relatively stable compared with other algorithms, and this is also reflected in Table IV.

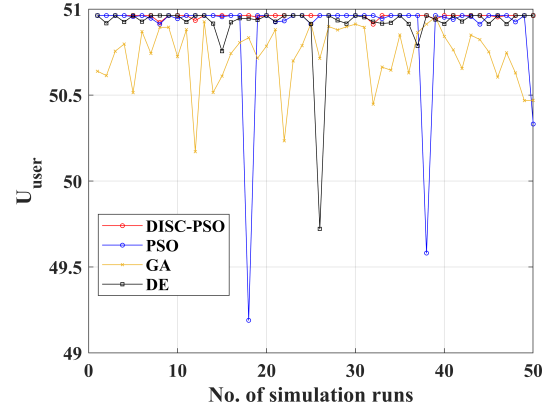


Fig. 7: P under different algorithms.

In addition, DISC-PSO has the lowest standard deviation on U_{user} , which further verifies the stability of the proposed algorithm.

Fig. 8 shows the number of iterations required to iterate to a qualified U_{user} , and we set the maximum number of iterations to 50. It is observed that DISC-PSO satisfies the condition of Eq.(32) in a few iterations. Compared with PSO, GA, and DE, the number of iterations decreased by 73.9%, 96.5%, and 83.2% respectively as shown in Table IV. This demonstrates that our proposed algorithm is highly efficient, achieving faster convergence with significantly fewer iterations.

As depicted in Fig. 9, we counted the convergence point distribution positions obtained by different algorithms after 50 simulation runs. Compared with other baseline algorithms, the point distribution of DISC-PSO is more concentrated and less. This means that the DISC-PSO can achieve relatively stable resource allocation and U_{user} , which helps the ES more accurately to predict the amount of resources that should be allocated to the EU, thereby ensuring rationality and fairness in resource allocation.

⁴Only the unrepeated points are drawn.

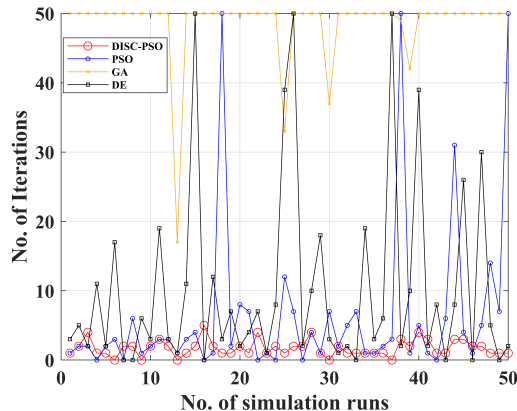


Fig. 8: The number of iterations under different algorithms.

TABLE IV: SUMMARY OF SIMULATION RESULTS OF DIFFERENT ALGORITHMS

Algorithm	Average U_{user}	Std	Average No. of iterations
DISC-PSO	50.96	0.01019	1.72
PSO	50.88	0.3232	6.58
GA	50.73	0.1732	48.56
DE	50.91	0.1765	10.24

V. CONCLUSION

In this paper, we develop a dynamic pricing based near-optimal resource allocation scheme and validate its effectiveness through extensive simulation results. Specifically, we derive utility functions for both EUs and ESs based on the proposed pricing scheme. Our theoretical analysis demonstrates that the EU utility function reaches a local maximum within the search range, which facilitates optimal resource allocation. Moreover, we find that near the local maximum, more resource allocation results in only modest improvements in utility. Therefore, to develop a more rational resource allocation scheme, we propose the DISC-PSO algorithm to identify a near-optimal allocation quantity. The effectiveness of the DISC-PSO algorithm is further validated by examining factors such as the number of iterations, average utility, standard deviation of utility, and resource distribution. In our future work, we will explore more dynamic factors and implement the proposed scheme into real-world experiments for practical validation.

APPENDIX A

The Hessian matrix \mathcal{H} for U_{user} is shown below.

$$\mathcal{H} = \begin{bmatrix} -\frac{2w_2cq}{F_{server}^3} & 0 \\ 0 & -\frac{2q\mathcal{Y}}{B^3} \end{bmatrix}. \quad (37)$$

Since \mathcal{H} is a diagonal matrix, we can get its eigenvalues λ_1 and λ_2 as shown below.

$$\begin{cases} \lambda_1 = -\frac{2w_2cq}{F_{server}^3}, \\ \lambda_2 = -\frac{2q\mathcal{Y}}{B^3}. \end{cases} \quad (38)$$

Because

$$\begin{cases} w_2 > 0, \\ c > 0, \\ q > 0, \\ F_{server} > 0, \\ B > 0, \end{cases} \quad (39)$$

$\lambda_1 < 0$. In addition, we know $\mathcal{Y} = \frac{w_1 P_u + w_2}{\log_2(1 + (\frac{S}{N})_{uplink})} + \frac{w_1 P_d \alpha + w_2 \alpha}{\log_2(1 + (\frac{S}{N})_{downlink})}$ (i.e., Eq.(17)). Since

$$\begin{cases} w_1 > 0, \\ P_u > 0, \\ P_d > 0, \\ \alpha > 0, \\ \log_2(1 + \mathcal{D}) > 0, \end{cases} \quad (40)$$

where $\mathcal{D} > 0$ is the signal to noise ratio, $\mathcal{Y} > 0$. Therefore, $\lambda_2 < 0$.

To sum up, since the eigenvalues λ_1 and λ_2 are both greater than zero, the \mathcal{H} is a negative definite matrix.

APPENDIX B

Denote $U_{user} = f(F_{server}, B)$. From Eq.(26), we know that $f(F_{server}, B)$ has a local maximum. We assume the local maximum point is (F_{server}^0, B^0) . In addition, the Hessian matrix \mathcal{H} at this point is negative definite, with the gradient $\nabla f(F_{server}^0, B^0) = 0$. The second-order Taylor expansion is expressed as:

$$\begin{aligned} f(F_{server}, B) &\approx f(F_{server}^0, B^0) \\ &+ \frac{1}{2} \begin{pmatrix} F_{server} - F_{server}^0 \\ B - B^0 \end{pmatrix}^T \mathcal{H} \begin{pmatrix} F_{server} - F_{server}^0 \\ B - B^0 \end{pmatrix}. \end{aligned} \quad (41)$$

Let the eigenvalues of the Hessian matrix \mathcal{H} as λ_1 and λ_2 . We use the eigenvectors v_1 and v_2 to present the corresponding eigenvalues. The vector $z = \begin{pmatrix} F_{server} - F_{server}^0 \\ B - B^0 \end{pmatrix}$ can be expressed as a linear combination of the eigenvectors:

$$z = c_1 v_1 + c_2 v_2, \quad (42)$$

where c_1 and c_2 are the coefficients representing the vector z in terms of the eigenvector basis v_1 and v_2 .

In this expression, the quadratic form $z^T \mathcal{H} z$ can be simplified as:

$$z^T \mathcal{H} z = \lambda_1 c_1^2 + \lambda_2 c_2^2. \quad (43)$$

Therefore, the quadratic approximation formula is:

$$f(F_{server}, B) \approx f(F_{server}^0, B^0) + \frac{1}{2}(\lambda_1 c_1^2 + \lambda_2 c_2^2). \quad (44)$$

Since λ_1 and λ_2 are negative, this expression becomes:

$$f(F_{server}, B) \approx f(F_{server}^0, B^0) - \frac{1}{2}(|\lambda_1|c_1^2 + |\lambda_2|c_2^2). \quad (45)$$

Here, we obtain the sizes of the eigenvalues λ_1 and λ_2 by substituting the simulation parameters in Table III. Thus, λ_1 and λ_2 are approximately 10^{-18} and 10^{-13} , respectively. Since

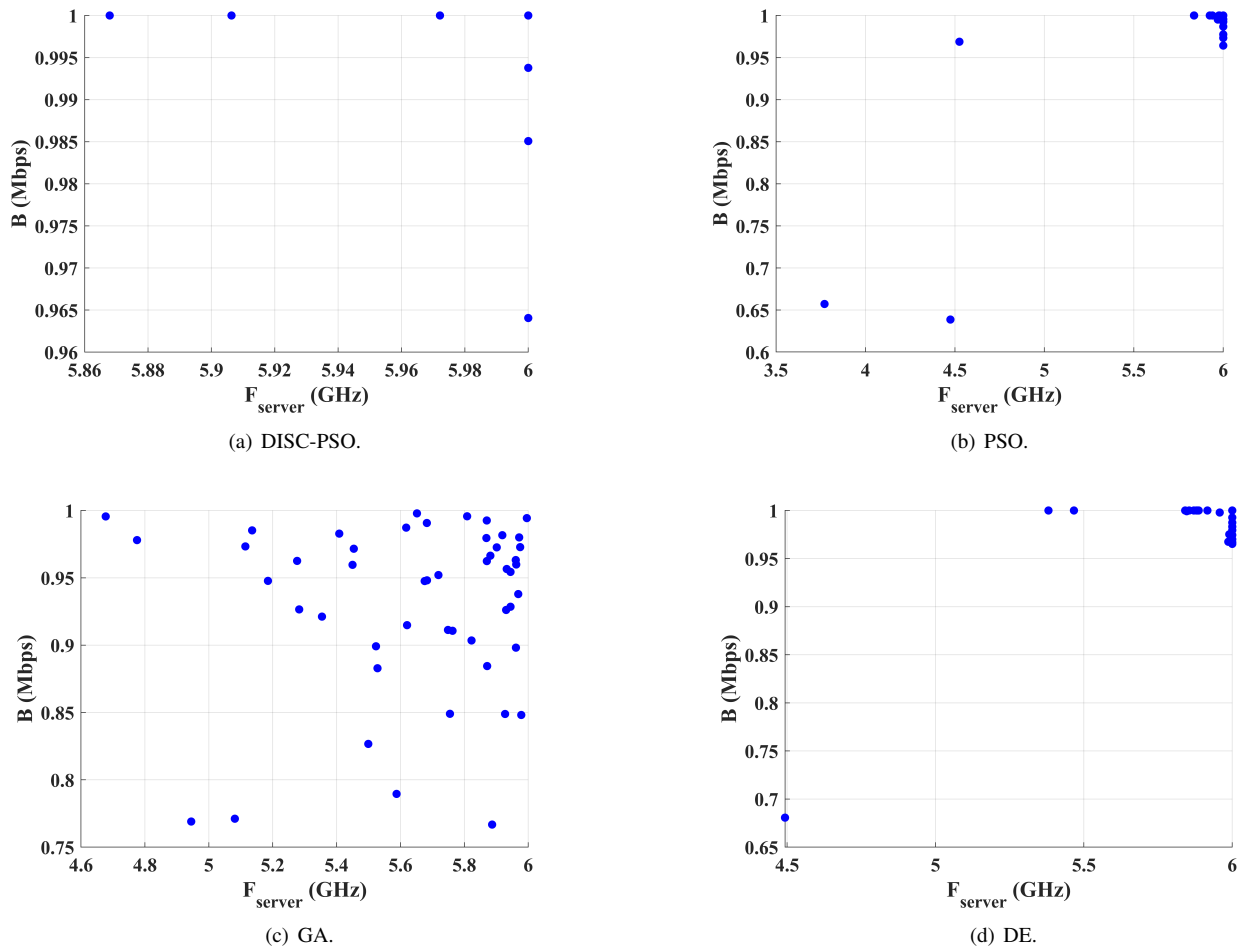


Fig. 9: Distribution of near-optimal points under different algorithms.⁴

λ_1 and λ_2 are very small, that is, $|\lambda_1|$ and $|\lambda_2|$ are very small positive number. This means:

$$|f(F_{server}, B) - f(F_{server}^0, B^0)| = \left| -\frac{1}{2}(|\lambda_1|c_1^2 + |\lambda_2|c_2^2) \right|. \quad (46)$$

Since $|\lambda_1|$ and $|\lambda_2|$ are very small, even if c_1 and c_2 are not particularly small⁵, $|\lambda_1|c_1^2 + |\lambda_2|c_2^2$ will be very small. Therefore, the overall change in the function value will be still very small.

In summary, since the eigenvalues λ_1 and λ_2 of the Hessian matrix are very small, the function value decreases very slowly near the local maximum (F_{server}^0, B^0) . This is because the descent term $\frac{1}{2}(|\lambda_1|c_1^2 + |\lambda_2|c_2^2)$ in the quadratic approximation formula does not significantly change the function value when $|\lambda_1|$ and $|\lambda_2|$ are very small. Therefore, the rate of descent of the function near the local maximum is slow. When the eigenvalues $|\lambda_1|$ and $|\lambda_2|$ are small, the curvature of the function in these directions is small, so the value of the function drops very slowly near the local maximum.

⁵The sizes of c_1 and c_2 determine how far the point (F_{server}, B) is from the point (F_{server}^0, B^0) . The smaller c_1 and c_2 are, the closer the two points are.

APPENDIX C

We analyzed some of the data in Fig. 2⁶, as shown in Table V. From the table, we can see that ΔU_{user} is twice as large as ΔU_{server} under the same conditions. In addition, when Eq. (32) is satisfied, the algorithm stops iteration. Let's make the following formula true.

$$\frac{U_{user}^{max} - S_{gb}}{S_{gb}} = \epsilon, \quad (47)$$

$$S_{gb} = \frac{U_{user}^{max}}{1 + \epsilon}.$$

Since $U_{user}^{max} - S_{gb} = \Delta U_{user}$, substituting this into Eq.(47)

⁶We have omitted the analysis of Fig. 3 data here. Fig. 3 shows that with an increase in B , the U_{server} is basically unchanged. Our goal is to omit the U_{server} analysis, which means we only need to consider the U_{user} . Therefore, only the U_{server} and U_{user} under different F is analyzed here, and the utility analysis under different B is omitted.

to get the following formulas.

$$\begin{aligned}\frac{\Delta U_{user}}{S_{gb}} &= \epsilon, \\ \Delta U_{user} &= \frac{\epsilon U_{user}^{max}}{1 + \epsilon}, \\ \Delta U_{user} &= \frac{U_{user}^{max}}{1 + \frac{1}{\epsilon}}.\end{aligned}\quad (48)$$

When $\epsilon \rightarrow 0$, $\Delta U_{user} \rightarrow 0$. Since $\Delta U_{server} = \frac{1}{2} \Delta U_{user}$, it follows that $\Delta U_{server} \rightarrow 0$. Thus, we can conclude that when U_{user} satisfies the stopping condition of the iteration and reaches its sub-maximum value, U_{server} also reaches its sub-maximum value. Therefore, we only need to discuss one of the cases. If we let U_{user} reach its sub-optimal value, then U_{server} will also correspondingly reach its sub-optimal value.

TABLE V: ΔU for different F_{server} ⁷

	ΔU_{21}	ΔU_{32}	ΔU_{43}	ΔU_{54}	ΔU_{65}
U_{user}	5.4067	1.8032	0.9011	0.5407	0.3604
U_{server}	2.70336	0.90112	0.45056	0.27034	0.18022

REFERENCES

- [1] G. Zhang, Y. Chen, Z. Shen, and L. Wang, "Distributed energy management for multiuser mobile-edge computing systems with energy harvesting devices and QoS constraints," *IEEE Internet Things J.*, vol. 6, no. 3, pp. 4035-4048, Jun. 2019.
- [2] M. Wazid, A. K. Das, V. Odelu, N. Kumar, and W. Susilo, "Secure remote user authenticated key establishment protocol for smart home environment," *IEEE Trans. Dependable Secure Comput.*, vol. 17, no. 2, pp. 391-406, Mar.-Apr. 2020.
- [3] Y. Sun, Z. Wu, K. Meng, and Y. Zheng, "Vehicular task offloading and job scheduling method based on cloud-edge computing," *IEEE Trans. Intell. Transp. Syst.*, vol. 24, no. 12, pp. 14651-14662, Dec. 2023.
- [4] M. Teng, X. Li, and K. Zhu, "Joint optimization of sequential task offloading and service deployment in end-edge-cloud system for energy efficiency," *IEEE Trans. Sustainable Comput.*, vol. 9, no. 3, pp. 283-298, May-Jun. 2024.
- [5] A. Bozorgchenani, F. Mashhadi, D. Tarchi, and S. A. Salinas Monroy, "Multi-objective computation sharing in energy and delay constrained mobile edge computing environments," *IEEE Trans. Mob. Comput.*, vol. 20, no. 10, pp. 2992-3005, Oct. 2021.
- [6] F. Fang, Y. Xu, Z. Ding, C. Shen, M. Peng, and G. K. Karagiannidis, "Optimal resource allocation for delay minimization in NOMA-MEC networks," *IEEE Trans. Commun.*, vol. 68, no. 12, pp. 7867-7881, Dec. 2020.
- [7] K. Guo, R. Gao, W. Xia, and T. Q. S. Quek, "Online learning based computation offloading in MEC systems with communication and computation dynamics," *IEEE Trans. Commun.*, vol. 69, no. 2, pp. 1147-1162, Feb. 2021.
- [8] G. Li, J. Cai, X. Chen, and Z. Su, "Nonlinear online incentive mechanism design in edge computing systems with energy budget," *IEEE Trans. Mob. Comput.*, vol. 22, no. 7, pp. 4086-4102, Jul. 2023.
- [9] G. Li and J. Cai, "An online incentive mechanism for collaborative task offloading in mobile edge computing," *IEEE Trans. Wireless Commun.*, vol. 19, no. 1, pp. 624-636, Jan. 2020.
- [10] J. Liu, S. Guo, K. Liu, and L. Feng, "Resource provision and allocation based on microeconomic theory in mobile edge computing," *IEEE Trans. Serv. Comput.*, vol. 15, no. 3, pp. 1512-1525, May-Jun. 2022.
- [11] C. Jiang, Z. Luo, L. Gao, and J. Li, "A truthful incentive mechanism for movement-aware task offloading in crowdsourced mobile edge computing systems," *IEEE Internet Things J.*, vol. 11, no. 10, pp. 18292-18305, May. 2024.
- [12] Y. Su, W. Fan, Y. Liu, and F. Wu, "A truthful combinatorial auction mechanism towards mobile edge computing in industrial internet of things," *IEEE Trans. Cloud Comput.*, vol. 11, no. 2, pp. 1678-1691, Apr.-Jun. 2023.
- [13] P. -Q. Huang, Y. Wang, and K. Wang, "A divide-and-conquer bilevel optimization algorithm for jointly pricing computing resources and energy in wireless powered MEC," *IEEE Trans. Cybern.*, vol. 52, no. 11, pp. 12099-12111, Nov. 2022.
- [14] T. Zhou, X. Zeng, D. Qin, N. Jiang, X. Nie, and C. Li, "Cost-aware computation offloading and resource allocation in ultra-dense multi-cell, multi-user and multi-task MEC networks," *IEEE Trans. Veh. Technol.*, vol. 73, no. 5, pp. 6642-6657, May 2024.
- [15] Y. Teng, K. Cheng, Y. Zhang, and X. Wang, "Mixed-timescale joint computational offloading and wireless resource allocation strategy in energy harvesting multi-MEC server systems," *IEEE Access*, vol. 7, pp. 74640-74652, 2019.
- [16] Z. Xiang, Y. Zheng, Z. Zheng, S. Deng, M. Guo, and S. Dustdar, "Cost-effective traffic scheduling and resource allocation for edge service provisioning," *IEEE/ACM Trans. Networking*, vol. 31, no. 6, pp. 2934-2949, Dec. 2023.
- [17] S. Cheng, T. Ren, H. Zhang, J. Huang, and J. Liu, "A Stackelberg-game-based framework for edge pricing and resource allocation in mobile edge computing," *IEEE Internet Things J.*, vol. 11, no. 11, pp. 20514-20530, Jun. 2024.
- [18] J. Ahmed, M. A. Razzaque, M. M. Rahman, S. A. Alqahtani, and M. M. Hassan, "A Stackelberg game-based dynamic resource allocation in edge federated 5G network," *IEEE Access*, vol. 10, pp. 10460-10471, 2022.
- [19] Y. Li, B. Yang, H. Wu, Q. Han, C. Chen, and X. Guan, "Joint offloading decision and resource allocation for vehicular fog-edge computing networks: a contract-Stackelberg approach," *IEEE Internet Things J.*, vol. 9, no. 17, pp. 15969-15982, Sept. 2022.
- [20] U. Habiba, S. Maghsudi, and E. Hossain, "A repeated auction model for load-aware dynamic resource allocation in multi-access edge computing," *IEEE Trans. Mob. Comput.*, vol. 23, no. 7, pp. 7801-7817, Jul. 2024.
- [21] W. Sun, J. Liu, Y. Yue, and H. Zhang, "Double auction-based resource allocation for mobile edge computing in industrial internet of things," *IEEE Trans. Ind. Inf.*, vol. 14, no. 10, pp. 4692-4701, Oct. 2018.
- [22] T. Bahreini, H. Badri, and D. Grosu, "Mechanisms for resource allocation and pricing in mobile edge computing systems," *IEEE Trans. Parallel Distrib. Syst.*, vol. 33, no. 3, pp. 667-682, Mar. 2022.
- [23] X. Wang, D. Wu, X. Wang, R. Zeng, L. Ma, and R. Yu, "Truthful auction-based resource allocation mechanisms with flexible task offloading in mobile edge computing," *IEEE Trans. Mob. Comput.*, vol. 23, no. 5, pp. 6377-6391, May 2024.
- [24] Z. Li, C. Jiang, and L. Kuang, "Double auction mechanism for resource allocation in satellite MEC," *IEEE Trans. Cognit. Commun. Networking*, vol. 7, no. 4, pp. 1112-1125, Dec. 2021.
- [25] Q. Li, H. Yao, T. Mai, C. Jiang, and Y. Zhang, "Reinforcement-learning-and belief-learning-based double auction mechanism for edge computing resource allocation," *IEEE Internet Things J.*, vol. 7, no. 7, pp. 5976-5985, Jul. 2020.
- [26] X. Huang, T. Huang, W. Zhang, C. K. Yeo, S. Zhao, and G. Zhang, "Pricing optimization in MEC systems: maximizing resource utilization through joint server configuration and dynamic operation," *IEEE Trans. Mob. Comput.*, vol. 23, no. 5, pp. 5863-5879, May 2024.
- [27] R. Wang, C. Zang, P. He, Y. Cui, and D. Wu, "Auction pricing-based task offloading strategy for cooperative edge computing," in *Proc. IEEE Glob. Commun. Conf. (GLOBECOM)*, Dec. 2021, pp. 1-6.
- [28] L. Li, T. Q. S. Quek, J. Ren, H. H. Yang, Z. Chen, and Y. Zhang, "An incentive-aware job offloading control framework for multi-access edge computing," *IEEE Trans. Mob. Comput.*, vol. 20, no. 1, pp. 63-75, Jan. 2021.
- [29] H. Seo, H. Oh, J. K. Choi, and S. Park, "Differential pricing-based task offloading for delay-sensitive IoT applications in mobile edge computing system," *IEEE IoT J.*, vol. 9, no. 19, pp. 19116-19131, Oct. 2022.
- [30] X. Wang, Y. Han, H. Shi, and Z. Qian, "JOAGT: latency-oriented joint optimization of computation offloading and resource allocation in D2D-assisted MEC system," *IEEE Wireless Commun. Lett.*, vol. 11, no. 9, pp. 1780-1784, Sept. 2022.
- [31] P. Xu, H. Zhou, X. Liu, J. Zhou, and Y. Yang, "Global optimizing prestack seismic inversion approach using an accurate Hessian Matrix based on exact zoeppritz equations," *IEEE Trans. Geosci. Remote Sens.*, vol. 62, pp. 1-16, 2024, Art no. 5907916.
- [32] L. Ma, C. Hu, J. Yu, L. Wang, and H. Jiang, "Distributed fixed/preassigned-time optimization based on piecewise power-law design," *IEEE Trans. Cybern.*, vol. 53, no. 7, pp. 4320-4333, Jul. 2023.
- [33] H. Zhang, Y. Xiao, S. Bu, D. Niyato, R. Yu, and Z. Han, "Fog computing in multi-tier data center networks: a hierarchical game approach," in *Proc. IEEE Int. Conf. Commun. (ICC)*, May 2016, pp. 1-6.

⁷ ΔU_{21} represents the increase in utility from point (1, U) to point (2, U), and so on.

- [34] B. Liang, R. Fan, H. Hu, Y. Zhang, N. Zhang, and A. Anpalagan, "Nonlinear pricing based distributed offloading in multi-user mobile edge computing," *IEEE Trans. Veh. Technol.*, vol. 70, no. 1, pp. 1077-1082, Jan. 2021.
- [35] T. Lyu, H. Xu, and Z. Han, "Multi-leader multi-follower Stackelberg game based resource allocation in multi-access edge computing," in *Proc. IEEE Int. Conf. Commun. (ICC)*, May 2022, pp. 4306-4311.
- [36] T. D. Tran and L. B. Le, "Resource allocation for multi-tenant network slicing: a multi-leader multi-follower Stackelberg game approach," *IEEE Trans. Veh. Technol.*, vol. 69, no. 8, pp. 8886-8899, Aug. 2020.
- [37] K. Wang, F. C. M. Lau, L. Chen, and R. Schober, "Pricing mobile data offloading: a distributed market framework," *IEEE Trans. Wireless Commun.*, vol. 15, no. 2, pp. 913-927, Feb. 2016.
- [38] M. Tao, K. Ota, M. Dong, and H. Yuan, "Stackelberg game-based pricing and offloading in mobile edge computing," *IEEE Wireless Commun. Lett.*, vol. 11, no. 5, pp. 883-887, May 2022.
- [39] U. Habiba, S. Maghsudi, and E. Hossain, "A reverse auction model for efficient resource allocation in mobile edge computation offloading," in *Proc. IEEE Glob. Commun. Conf. (GLOBECOM)*, 2019, pp. 1-6.
- [40] M. Liu and Y. Liu, "Price-based distributed offloading for mobile-edge computing with computation capacity constraints," *IEEE Wireless Commun. Lett.*, vol. 7, no. 3, pp. 420-423, Jun. 2018.
- [41] L. Li, M. Siew, Z. Chen, and T. Q. S. Quek, "Optimal pricing for job offloading in the MEC system with two priority classes," *IEEE Trans. Veh. Technol.*, vol. 70, no. 8, pp. 8080-8091, Aug. 2021.



Yun Xia received the B.S. degree from Shanghai Ocean University, Shanghai, China, in 2022. He is currently working toward the master's degree in computer science and technology with the University of Shanghai for Science and Technology, Shanghai, China. His research focuses on mobile edge computing and pricing strategy.



Hai Xue (Member, IEEE) received the B.S. degree from Konkuk University, Seoul, South Korea, in 2014, the M.S. degree from Hanyang University, Seoul, South Korea, in 2016, and the Ph.D. degree from Sungkyunkwan University, Suwon, South Korea, in 2020. He is currently an assistant professor at the School of Optical-Electrical and Computer Engineering, University of Shanghai for Science and Technology (USST), Shanghai, China. Prior to joining USST, he was a research professor with the Mobile Network and Communications Lab. at Korea

University from 2020 to 2021, Seoul, South Korea. His research interests include edge computing/intelligence, SDN/NFV, machine learning, and swarm intelligence.



Di Zhang (Senior Member, IEEE) is currently an Associate Professor with Zhengzhou University. His research interests include wireless communications and networking, especially the short packet communications and its applications. He received the ITU Young Author Recognition in 2019, the First Prize Award for Science and Technology Progress of Henan Province in 2023, and the First Prize Award for Science and Technology Achievements from the Henan Department of Education in 2023. He is serving as an Area Editor for KSII Transactions on

Internet and Information Systems, and has served as the Guest Editor for IEEE WIRELESS COMMUNICATIONS and IEEE NETWORK.



Shahid Mumtaz (Senior Member, IEEE) is an IET Fellow, the IEEE ComSoc Lecturer, and an ACM Distinguished Speaker. He has authored 4 technical books, 12 book chapters, and more than 300 technical articles (more than 200 IEEE Journals/Transactions, more than 100 conferences, and two IEEE best paper awards) in mobile communications. Dr. Mumtaz is the recipient of the NSFC Researcher Fund for Young Scientist in 2017 from China, and the IEEE ComSoc Young Researcher Award in 2020. He was awarded an Alain Bensoussan Fellowship in 2012. He is the Founder and EiC of IET Journal of quantum Communication, the Vice Chair of Europe/Africa Region—IEEE ComSoc: Green Communications & Computing society, and the IEEE standard on P1932.1: Standard for Licensed/Unlicensed Spectrum Interoperability in Wireless Mobile Networks.



Xiaolong Xu (Senior Member, IEEE) received the Ph.D. degree in computer science and technology from Nanjing University, China, in 2016. He is currently a Full Professor with the School of Software, Nanjing University of Information Science and Technology. He has published more than 100 peer-review articles in international journals and conferences, including the IEEE TKDE, IEEE TPDS, JSAC, IEEE TSC, SCIS, IEEE TFS, IEEE T-ITS, ACM SIGIR, IJCAI, ICDM, ICWS, ICSOC, etc. He was selected as the Highly Cited Researcher of

Clarivate (2021-2023). He received best paper awards from Tsinghua Science and Technology at 2023, Journal of Network and Computer Applications at 2022, and several conferences, including IEEE HPCC 2023, IEEE ISPA 2022, IEEE CyberSciTech 2021, IEEE CPSCom2020, etc. His research interests include edge computing, the Internet of Things (IoT), cloud computing, and big data.



Joel J. P. C. Rodrigues (Fellow, IEEE) is currently the Leader of the Center for Intelligence, Fecomrcio/CE, Brazil, and a Full Professor with COPELABS, Lusófona University, Lisbon, Portugal. He is also a Highly Cited Researcher (Clarivate), No. 1 of the top scientists in computer science in Brazil (Research.com), the Leader of the Next Generation Networks and Applications (NetGNA) Research Group (CNPq), a Member Representative of the IEEE Communications Society on the IEEE Biometrics Council, and the President of the Scientific Council at ParkUrbis Science and Technology Park. He has authored or coauthored about 1150 papers in refereed international journals and conferences, three books, two patents, and one ITU-T Recommendation.

He was the Director of Conference Development—IEEE ComSoc Board of Governors, an IEEE Distinguished Lecturer, a Technical Activities Committee Chair of the IEEE ComSoc Latin America Region Board, the past Chair of the IEEE ComSoc Technical Committee (TC) on eHealth and the TC on Communications Software, a Steering Committee Member of the IEEE Life Sciences Technical Community, and the publications co-chair. He is a member of the Internet Society, a senior member ACM, and a fellow of AAIA. He had been awarded several Outstanding Leadership and Outstanding Service Awards by IEEE Communications Society and several best papers awards. He is the Editor-in-Chief of the *International Journal of E-Health and Medical Communications* and an editorial board member of several high reputed journals.